

Electron-phonon coupling in single walled carbon nanotubes determined by shot noise

F. Wu,¹ P. Virtanen,¹ S. Andresen,² B. Placais,³ and P.J. Hakonen¹

¹*Low Temperature Laboratory, Aalto University, Espoo, Finland*

²*Niels Bohr Institute, University of Copenhagen, 2100 København Ø, Denmark*

³*Ecole Normale Supérieure, Laboratoire Pierre Aigrain,
24 rue Lhomond, 75005 Paris, France*

(Dated: December 5, 2018)

Abstract

We have measured shot noise in metallic single-walled carbon nanotubes of length $L = 1 \mu\text{m}$ and have found strong suppression of noise with increasing voltage. We conclude that the coupling of electron and phonon baths at temperatures T_e and T_{ph} is described at intermediate bias ($20 \text{ mV} < V_{ds} \lesssim 200 \text{ mV}$) by heat flow equation $P = \Sigma L(T_e^3 - T_{ph}^3)$ where $\Sigma \sim 3 \cdot 10^{-9} \text{ W/mK}^3$ due to electron interaction with acoustic phonons, while at higher voltages optical phonon - electron interaction leads to $P = \kappa_{op} L [N(T_e) - N(T_{ph})]$ where $N(T) = 1/(\exp(\hbar\Omega/k_B T) - 1)$ with optical phonons energy $\hbar\Omega$ and $\kappa_{op} = 2 \cdot 10^2 \text{ W/m}$.

PACS numbers: PACS numbers: 73.63.Fg, 63.20.kd, 65.80.Ck

Theoretical models based on mean-free path type of arguments have successfully been employed to explain experimental current-voltage characteristics of single-walled carbon nanotubes (SWNTs), and they indicate optical phonon generation with high phonon temperatures in measurements at large bias voltages [1–5]. In addition, time-resolved photoelectron spectroscopy has been used to probe energy relaxation between electrons and phonons in carbon nanotubes [6, 7]. Recently, high-bias electron transport studies in conjunction with Raman spectroscopy have been performed and direct confirmation of the high phonon temperatures of several hundred Kelvin has been obtained [8, 9].

These investigations have addressed only the phonon temperature and the electronic temperature has not been determined. We have studied shot noise in single-walled nanotubes at high bias and employed the noise to determine the electronic temperature. Assuming that acoustic phonons remain at the substrate temperature, we can determine the relation for the heat flux between electron and phonon baths in SWNTs [10]. We compare our results with those obtained by Raman spectroscopy and find close agreement with the reported optical phonon temperatures.

For large electron-phonon (e-ph) or electron-electron scattering rates, the solutions of the diffusive Boltzmann equation tend towards a Fermi function, i.e., to a local equilibrium [11]: $f(\varepsilon, \mathbf{x}) \approx f_0(\varepsilon, V(\mathbf{x}), T(\mathbf{x})) \equiv \frac{1}{e^{(\varepsilon-V(\mathbf{x}))/T(\mathbf{x})}+1}$, characterized by a local potential $V(\mathbf{x})$ and a temperature $T(\mathbf{x})$. Considering a 1D wire this yields for the Fano factor

$$\begin{aligned} \mathfrak{F} &\equiv \frac{S_I}{2eI} = \frac{2k_B}{LeV} \int_0^L dx \int_{-\infty}^{\infty} d\varepsilon f(\varepsilon, x)[1 - f(\varepsilon, x)] \\ &= \frac{2k_B}{LeV} \int_0^L dx T(x) \equiv \frac{2k_B T_e}{eV}, \end{aligned} \quad (1)$$

where S_I denotes the shot noise power and T_e is the average electronic temperature. If thermal conduction is dominated by electronic conduction, the Boltzmann equation yields with the phonon bath at $T_{ph} = 0$: $T_e = \frac{\sqrt{3}}{8} \frac{eV}{k_B}$ and $\mathfrak{F} = \frac{\sqrt{3}}{4}$, the well-known theoretical estimate due to hot electrons at an internal equilibrium [12].

Besides the electronic heat conduction $P_{\text{diff}} = \frac{\pi^2}{3} \frac{k_B^2}{e^2} T(x) \frac{dT(x)}{dx}$, power flow P_{inel} between electrons and phonons has to be taken into account when determining $T(x)$ [13]. We have considered the standard energy balance model for the electron-sample phonon-substrate coupling, described for example in Fig. 1 of Ref. 14, in which the Joule heating P_{Joule} dissipates either to the diffusive reservoir P_{diff} or to the lattice via inelastic scattering P_{inel} . In such a model, the relative magnitude of P_{diff} to P_{inel} determines the magnitude of the noise: $(eV)^2 - \frac{64}{3}(k_B T_e)^2 = \frac{1}{\epsilon_{\text{Th}}} P_{\text{inel}}(T_e)$, valid in the limit $T_{ph} \rightarrow 0$; here $\epsilon_{\text{Th}} =$ denotes

Thouless energy. In Ref. [15] the configuration for a typical nanotube sample is analyzed. Its conclusion is that, at intermediate voltages, the electron-phonon heat transfer is the bottleneck and, consequently, shot noise can be employed to obtain information on e-ph coupling.

For the dissipated power P_{inel} via e-ph interaction with Debye-like acoustic phonon spectrum [16], one obtains when Debye temperature $\theta_D = \hbar\omega_D/k_B \gg T$ (see also [10]):

$$P_{\text{inel}} = \Sigma L [T^{\alpha+3} - T_{ph}^{\alpha+3}] \quad (2)$$

where Σ specifies the strength of the e-ph interaction per unit length, and the exponent $\alpha = 0$ for a 1D sample. In general, α depends on the dimensionality of the electron and phonon systems, disorder and possibly on other factors [17, 18].

For a single band of optical phonons with energy $\hbar\Omega$, P_{inel} is given by

$$P_{\text{inel}} = \kappa_{op} [\coth(\frac{\hbar\Omega}{2k_B T}) - \coth(\frac{\hbar\Omega}{2k_B T_{ph}})], \quad (3)$$

where κ_{op} describes the strength of the interaction between electrons and acoustic phonons via optical phonon modes [19]: $\kappa_{op} = \kappa_{e-op}\kappa_{op-ac}/(\kappa_{e-op} + \kappa_{op-ac})$, where κ_{e-op} denotes the coupling between electrons and optical phonons and κ_{op-ac} governs the relaxation of optical phonon branches to acoustic phonons.

In voltage-biased nanotubes, the energy of electrons ε is supplied by the voltage V . From the Debye-like acoustic phonon scattering, one obtains $\mathfrak{F} \propto V^{-(\alpha+1)/(\alpha+3)}$, which yields $\mathfrak{F} \propto 1/V^{1/3}$ for a 1D conductor. For the e-op scattering, the behavior at large voltages can be approximated by the estimate

$$\mathfrak{F} = \frac{2(\hbar\Omega/eV)}{\ln[1 + \kappa_{op}/IV]}. \quad (4)$$

where we consider e-op coupling as the major relaxation channel.

Our nanotube samples were grown with chemical vapor deposition (CVD). They were manufactured on top of insulating sapphire substrates in order to minimize parasitic capacitance and to reduce RF losses. Pairs of 25/15 nm Ti/Au contacts, 0.3 μm apart, were patterned between the catalyst islands by electron beam lithography. A central top-gate, 0.1 μm wide, was deposited between the contacts. It consisted of an insulating barrier, formed by five 2 nm Al layers, each oxidized for 2 min at dry atmospheric conditions, followed by a 25-nm layer of Ti for the lead itself. The tube diameters were around 2 nm.

In our measurement setup at frequency $f = 600\text{--}950$ MHz, we use a liquid-helium-cooled low-noise amplifier (LNA) [20]. We determine the differential Fano factor $F_d = \frac{1}{2e} \frac{dS_I}{dI}$ using lock-in techniques, and obtain the average, excess noise Fano factor by $F = \frac{1}{I} \int_0^I F_d dI = (S_I(I) - S(0)) / (2eI)$ [21]. The nonlinearity of the IV curve of the SWNT is taken into account using the scheme described in Ref. 22. Our measured F is an approximation for the true Fano factor \mathfrak{F} because, with substantial V_{ds} -induced sample heating, the noise does not fully cross over to the shot noise regime: the correction factor is at most $\approx \coth \frac{2eV}{4k_B T} = \coth \frac{1}{\mathfrak{F}} \simeq 1$ within 5% when $F < 0.5$, the main region of interest in our analysis.

Fig. 1 displays the differential conductance $G_d = \frac{dI}{dV_{ds}}$ vs. bias voltage V_{ds} measured at $T_0 = 4.2$ K. Initially, there is rather strong Coulomb blockade that suppresses the conductance below a few millivolts. Above the Coulomb blockade $V_{ds} > 10$ mV, G_d increases gradually and reaches a maximum around $V_{ds} = 0.1\text{--}0.2$ V, above which G_d starts to decrease, in a manner similar to that found by Yao et al. [1]. As in Ref. 1, we model the decrease by generation of optical phonons. Moreover, this decrease in G_d suggests that the electrical contacts on our sample are reasonably good, since otherwise the decrease of conductance due to optical phonon scattering could not be observed according to Ref. 1. Our maximum conductance of $\sim 0.5 e^2/h$ (30% less than in Ref. 1) implies a mean free path of $l_e \sim 60$ nm. There is slight asymmetry in G_d data in Fig. 1, presumably due to universal conductance fluctuation (UCF) type of behavior.

The results of shot noise measurements $S_I(I)$ is illustrated in the inset of Fig. 1. Using the Khlus formula [23], we may fit to the data and find $\mathfrak{F} = 2$ at very small voltage ($V_{ds} < 5$ mV). Large \mathfrak{F} at low bias is a sign of cotunneling phenomena which are known to enhance shot noise in SWNTs [24]. At large bias, $V_{ds} > 0.5$ V (above $7 \mu\text{A}$ in the inset of Fig. 1), S_I tends to saturate, especially at negative bias voltages. This is similar to the behavior observed in semiconducting SWNTs [25].

Fig. 2 displays the Fano factor F vs. V_{ds} . Above the cotunneling maximum in F at $V_{ds} \sim 5$ mV (not shown), the Fano factor starts to decrease. The heat transfer is initially dominated by diffusion along the tube and the hot electron regime is approached. However, the hot-electron value $\mathfrak{F} = \frac{\sqrt{3}}{4}$ is not favored in Fig. 2. Consequently, we conclude that the noise decreases already at intermediate voltage $20 \text{ mV} < V_{ds} \lesssim 200 \text{ mV}$ due to inelastic processes. This finding signifies a relatively large inelastic scattering rate, which may be an indication of coupling to substrate modes [26]. At higher bias, power starts to flow out from

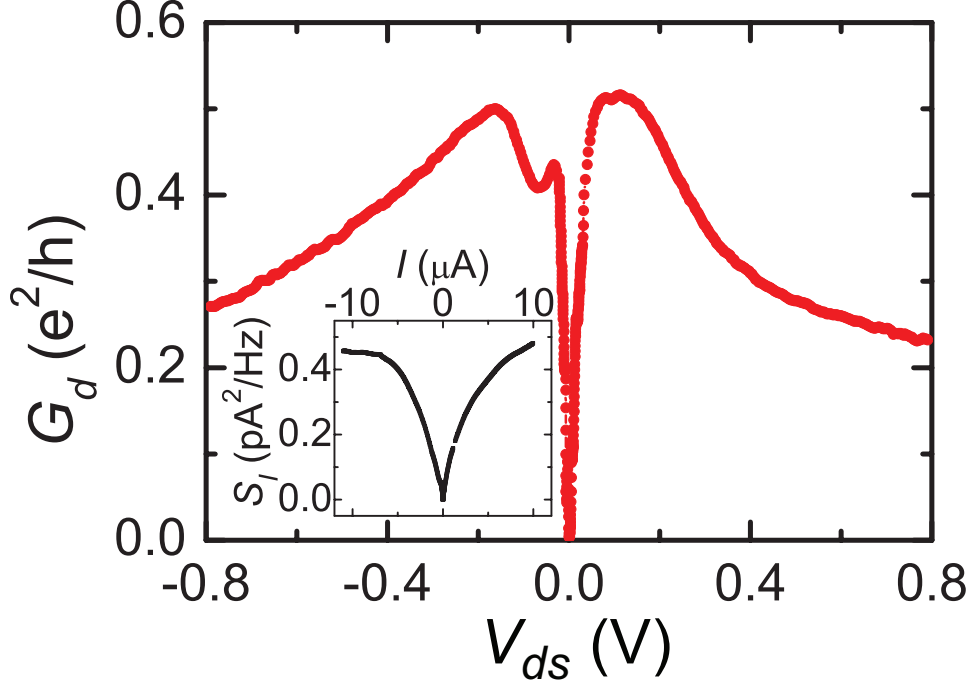


FIG. 1. (Color online) Differential conductance G_d of a typical SWNT nanotube sample recorded at $T = 4.2$ K. Measured power spectral density of current noise $S_I(I)$ is shown in inset.

the electronic system via electron-optical phonon coupling, and F is decreased even stronger. By fitting to the data in Fig. 2 we find $F \propto V_{ds}^{-0.6}$ at $V_{ds} > 100$ mV and $F \propto V_{ds}^{-0.45}$ at $V_{ds} < 100$ mV. Other samples yielded similar values at high bias whereas somewhat larger variation in the exponent was observed at $V_{ds} < 100$ mV. The semiclassical model with acoustic phonon scattering is thus only qualitatively consistent with our data. However, optical phonon scattering described by Eq. 4 is found to agree well with the high bias data at $V_{ds} \gtrsim 0.2$ V using $\kappa_{op} = 2 \cdot 10^2$ W/m).

Encouraged by the success of semiclassical modeling, we have employed our shot noise results for thermometry to determine the average electronic temperature T_e on the sample according to Eq. 1. Figure 3 displays the total heat flow due to dissipated power $P_{\text{Joule}} = IV_{ds}$ vs. T_e deduced from F . In order to estimate Σ and κ_{op} , we neglect P_{diff} , the contribution of which is small at high bias. A fit using $T_e^4 - T_{ph}^4$, with $T_{ph} = T_0$, would work the best over the whole range of data, consistent with an exponent of $\alpha = 1$ in the Debye-like spectrum. This would correspond to graphene-like 2-dim behavior [27] which could point towards strongly modified phonon modes by the presence of the SiO_2 substrate [26].

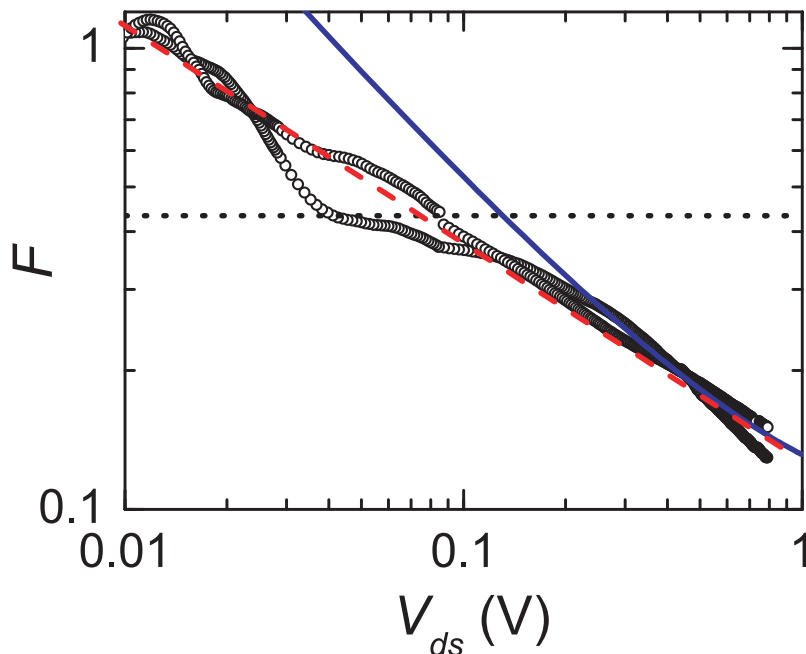


FIG. 2. (Color online) Fano factor F vs. absolute value of V_{ds} on log-log scale. $F \propto V_{ds}^{-0.45}$ is illustrated in the figure by the dashed line. The solid blue curve displays the fit of Eq. 4 to the data. The dotted line denotes the hot electron value for F .

At the intermediate bias range $20 \text{ mV} < V_{ds} \lesssim 200 \text{ mV}$ ($T_e \simeq 100 \text{ K}$), we are also able to fit the exponent $\alpha = 0$ with the data as seen by the red solid curve in Fig. 3. This yields $P_{inel} = \Sigma L(T^3 - T_0^3)$ with $\Sigma \sim 3 \cdot 10^{-9} \text{ W/mK}^3$. At $V_{ds} \gtrsim 0.2 \text{ V}$ ($T_e \gtrsim 350 \text{ K}$), optical phonons take over and we obtain a good fit of Eq. 3 to the data using $\kappa_{op} = 2 \cdot 10^2 \text{ W/m}$ and $\hbar\Omega = 0.18 \text{ eV}$. [28]. Our result displays a different power law compared with the work of Moos et al. [7] who obtain a relation of $T_e^5 - T_0^5$ for a nanotube bundle. Our low-bias dependence $P \propto T^3$ agrees with the result of Appenzeller *et al.* who report temperature dependence $\propto 1/T_e$ for the electron-phonon scattering time [29].

In conclusion, using diffusive transport theory and shot noise measurements in SWNTs at high bias, we determined the electronic temperature which nearly coincides with phonon temperatures obtained recently by Raman spectroscopy in Refs. 9, 26, and 30. Consequently, optical phonons and electrons are nearly at the same temperature, which is in agreement with standard heat flow modeling with typical electron-phonon coupling parameters [4].

We wish to thank V. Ermelov, T. Heikkilä, F. Mauri, N. Vandecasteele, and J. Viljas for

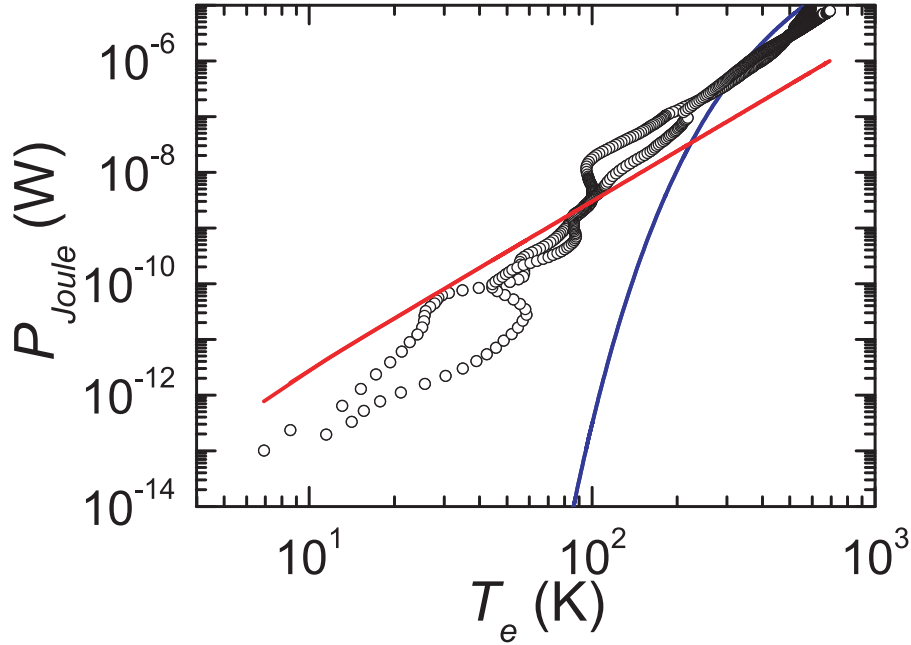


FIG. 3. (Color online) Joule heating $P_{\text{Joule}} = IV_{ds}$ vs. electronic temperature $T_e = \frac{FeV_{ds}}{2k_B}$. Theory curves for acoustic phonons from Eq. 2 ($\Sigma \sim 3 \cdot 10^{-9}$ W/mK³) and for optical phonons from Eq. 3 ($\kappa_{op} = 2 \cdot 10^2$ W/m) are illustrated by the red and blue solid curves, respectively.

useful discussions and correspondence. This work was supported by the Academy of Finland (Materials World Network), EU FP6-IST-021285-2, and the NANOSYSTEMS project with Nokia Research Center.

-
- [1] Z. Yao, C. L. Kane, and C. Dekker, Phys. Rev. Lett., **84**, 2941 (2000).
 - [2] E. Pop, D. Mann, J. Cao, Q. Wang, K. Goodson, and H. Dai, Phys. Rev. Lett., **95**, 155505 (2005).
 - [3] M. Lazzeri, S. Piscanec, F. Mauri, A. C. Ferrari, and J. Robertson, Phys. Rev. Lett., **95**, 236802 (2005).
 - [4] M. Lazzeri and F. Mauri, Phys. Rev. B, **73**, 165419 (2006).
 - [5] E. Pop, D. A. Mann, K. E. Goodson, and H. Dai, J. Appl. Phys., **101**, 093710 (2007).
 - [6] T. Hertel, R. Fasel, and G. Moos, Appl. Phys. A, **75**, 449 (2002).

- [7] G. Moos, R. Fasel, and T. Hertel, *J. Nanosci. Nanotechnol.*, **3**, 145 (2003).
- [8] A. W. Bushmaker, V. V. Deshpande, M. W. Bockrath, and S. B. Cronin, *Nano Letters*, **7**, 3618 (2007).
- [9] M. Oron-Carl and R. Krupke, *Phys. Rev. Lett.*, **100**, 127401 (2008).
- [10] P. B. Allen, *Phys. Rev. Lett.*, **59**, 1460 (1987).
- [11] M. R. Arai, *Appl. Phys. Lett.*, **42**, 906 (1983).
- [12] K. E. Nagaev, *Phys. Rev. B*, **52**, 4740 (1995).
- [13] R. Tarkiainen, M. Ahlskog, P. Hakonen, and M. Paalanen, in *Quantum transport and quantum coherence (Localization 2002)*, *J. Phys. Soc. Jpn., Suppl. A*, Vol. 72 (The Physical Society of Japan, 2003) p. 100.
- [14] F. C. Wellstood, C. Urbina, and J. Clarke, *Phys. Rev. B*, **49**, 5942 (1994).
- [15] [Http://ltd.tkk.fi/pauli/virtanen05mastersthesis.pdf](http://ltd.tkk.fi/pauli/virtanen05mastersthesis.pdf).
- [16] G. Bergmann, W. Wei, and Y. Zou, *Phys. Rev. B*, **41**, 7386 (1990).
- [17] A. Sergeev, M. Y. Reizer, and V. Mitin, *Phys. Rev. Lett.*, **94**, 136602 (2005).
- [18] J. T. Karvonen, L. J. Taskinen, and I. J. Maasilta, *Phys. Rev. B*, **72**, 12302 (2005).
- [19] W.-K. Tse and S. Das Sarma, *Phys. Rev. B*, **79**, 235406 (2009).
- [20] L. Roschier and P. Hakonen, *Cryogenics*, **44**, 783 (2004).
- [21] R. Danneau, F. Wu, M. F. Craciun, S. Russo, M. Y. Tomi, J. Salmilehto, A. F. Morpurgo, and P. J. Hakonen, *J. Low Temp. Phys.*, **153**, 374 (2008).
- [22] F. Wu, P. Queipo, A. Nasibulin, T. Tsuneta, T. Wang, E. Kauppinen, and P. Hakonen, *Phys. Rev. Lett.*, **99** (2007).
- [23] Y. A. Blanter and M. Büttiker, *Phys. Rep.*, **336**, 1 (2000).
- [24] E. Onac, F. Balestro, B. Trauzettel, C. F. J. Lodewijk, and L. P. Kouwenhoven, *Phys. Rev. Lett.*, **96**, 026803 (2006).
- [25] J. Chaste, E. Pallecchi, P. Morfin, G. Fève, T. Kontos, J.-M. Berroir, P. Hakonen, and B. Plaças, *Appl. Phys. Lett.*, **96**, 192103 (2010).
- [26] M. Steiner, M. Freitag, V. Perebeinos, J. C. Tsang, J. P. Small, M. Kinoshita, D. Yuan, J. Liu, and P. Avouris, *Nature Nanotechn.*, **4**, 320 (2009).
- [27] J. K. Viljas and T. T. Heikkilä, *Phys. Rev. B*, **81**, 245404 (2010).
- [28] Our shot noise results are not affected by contact resistance because if it were significant, then Fano factor would remain constant and the T -dependence in Fig. 3 would be like $P_{\text{inel}} \propto T_e^2$,

which does not agree with the observed behavior.

- [29] J. Appenzeller, R. Martel, P. Avouris, H. Stahl, and B. Lengeler, *Appl. Phys. Lett.*, **78**, 3313 (2001).
- [30] V. V. Deshpande, S. Hsieh, A. W. Bushmaker, M. Bockrath, and S. B. Cronin, *Phys. Rev. Lett.*, **102**, 105501 (2009).